科学通报
进 展
《中国科学》杂志社
SCIENCE CHINA PRESS

富锂层状正极材料产业化的关键挑战与进展

戴宗良[1], 乔羽[2*]

1. 山东大学澳国立联合理学院, 威海 264209
2. 厦门大学固体表面物理化学国家重点实验室, 厦门 361005
* 联系人, E-mail: yuqiao@xmu.edu.cn

2026-05-07 收稿, 2026-05-26 修回, 2026-06-22 接受, 2026-07-14 网络版发表
国家自然科学基金(22288102)资助

摘要 富锂层状正极材料由于其独特的阴离子氧化还原机制, 其理论比容量可超过300 mAh/g, 被视为下一代高能量密度锂离子电池最具潜力的正极材料. 然而, LRLO材料在实际应用中仍面临严重的容量、电压衰减、循环稳定性差以及与产业化配套协议的脱节等问题. 本文阐述了该领域近期的突出进展, 重点从前驱体工程、化成激活协议及实际应用中的放电深度(depth-of-discharge, DOD)三个核心维度展开讨论. 首先, 揭示了前驱体(碳酸盐vs.氢氧化物)通过改变一次初级颗粒的堆积密度(primary-particle stacking density, PSD)决定材料结构稳定性的深层机制; 其次, 阐明了初始循环化成电压对晶体配位环境(O4→O5转变)及过渡金属迁移的调控作用; 最后, 针对实际工况中低放电深度(LDOD)导致的异常容量衰减, 探讨了氧化态晶格氧积累的影响. 研究发现这些问题是因为晶格氧的不可逆氧化还原及其伴随的复杂结构演化. 本文归纳总结了富锂材料在结构演化与界面稳定性方面的最新成果, 并分析了其科学意义, 为加速富锂正极材料的产业化进程提供了从基础研究到应用策略的全面展望.

关键词 富锂层状正极材料, 前驱体, 初级颗粒的堆积密度, 化成电压, 放电深度

1 富锂层状正极材料的简介

近年来, 全球能源结构转型以及电动汽车市场的迅猛发展, 对高能量密度、长寿命、低成本的锂离子电池提出了前所未有的需求[1,2]. 但是目前商业化层状正极(如钴酸锂、镍钴锰酸锂)主要依赖过渡金属(transition metal, TM)阳离子氧化还原, 可用容量接近理论上限[3,4]. 现有正极材料难以满足未来更高性能的需求, 因此亟需新型正极体系以突破容量天花板[5,6]. 富锂层状氧化物(lithium-rich layered oxide, LRLO)正极材料兼具TM阳离子与晶格氧阴离子协同氧化还原机制, 可提供更高的可逆比容量和更大的比能量, 被认为是最具应用潜力的新一代高能量密度正极材料之一[7~10].

1.1 富锂层状正极材料的结构特点

得益于氧相关的阴离子氧化还原反应, 富锂层状氧化物展现出不同寻常的高放电比容量和高工作电压[11]. 具体来说, 过量的锂进入并取代了过渡金属层中的部分过渡金属位点, 促使材料由单一的层状结构(Li-O-M构型)演变为包含Li-O-M与Li-O-Li两种构型的富锂双相结构, 这种特殊的Li-O-Li构型中的Li 1s轨道与O 2p轨道之间存在较大的能量差而难以形成杂化轨道, 产生了孤立的O 2p非键轨道, 进而触发晶格氧的氧化还原活性[12,13]; 通过晶格氧参与电荷补偿过程, 富锂层状正极材料最终得以实现额外容量的提升[14,15].

引用格式: 戴宗良, 乔羽. 富锂层状正极材料产业化的关键挑战与进展. 科学通报
Dai Z, Qiao Y. Critical challenges and recent advances in the commercialization of lithium-rich layered cathodes (in Chinese). Chin Sci Bull, doi: 10.1360/CSB-2026-0653

© 2026《中国科学》杂志社

1.2 富锂层状正极材料的挑战

然而，LRLO的产业化进程仍面临诸多严峻挑战，包括严重的初始容量损失、循环过程中的电压衰减以及潜在的安全隐患[16~18]. 尽管学术界在通过离子掺杂、表面包覆及空位工程稳定LRLO晶体结构方面取得了显著进展，但许多基础且关键的产业化应用场景在实验室研究中仍常被忽视. 这种学术研究与工业实际之间的脱节，已成为阻碍富锂层状正极材料商业化应用的主要瓶颈. 本文从产业化角度出发，总结整理富锂层状正极材料在前驱体、化成电压、放电深度三大维度的研究进展，旨在揭示各因素间的耦合机理，填补机理分散与优化碎片化的空白. 为设计更具稳定性的LRLO、优化化成制度与制定合理使用工况提供理论与实践指导.

2 前驱体工程: 产业化的物理与结构基石

前驱体是影响富锂正极粉体微结构与可加工性的首要因素. 前驱体的形貌、初级颗粒的堆积密度(primary-particle stacking density, PSD)比表面积(specific surface area, SSA)以及元素均匀性等微观结构参数决定LRLO产物的晶体结构、二次颗粒形貌、界面特性以及锂离子扩散动力学，最终影响其电化学性能[19,20]. 层状氧化物正极前驱体主要包括碳酸盐前驱体($TMCO_3$)与氢氧化物前驱体($TM(OH)_x$)，二者在体积能量密度、成本效率、储存性能、适用性、界面稳定性上存在差异显著. 由碳酸盐前驱体制备的CO3-LRLO正极原料成本低、合成工艺简单、储存条件宽松，适合大规模工业化生产；但振实密度低、体积能量密度不足、电极/电解液界面稳定性差，易发生副反应. 氢氧化物前驱体制备的OH-LRLO正极原料成本高、合成工艺复杂、整体成本更高；且$TM(OH)_x$对空气中H_2O、CO_2敏感，储存时易吸湿分解，需严苛储存条件；但振实密度更高、体积能量密度充足、界面稳定性更优[21,22].

2.1 相演化差异与微观颗粒构筑参数(PSD与PAR)

由于阴离子基团的差异，$TMCO_3$与$TM(OH)_x$在与锂源混合后的高温固相合成中表现出截然不同的相演化路径与晶面生长倾向. 如图1(a)所示，采用原位高温X射线衍射(HT-XRD)研究25~850 ℃的高温固相合成过程. $TMCO_3$在低温(≤300 ℃)环境下先脱水脱碳释放出大量的CO_2气体，导致材料内部形成更多的孔隙，并经历$Li_xNiMn_2O_4$尖晶石中间相后形成层状结构，且更倾向于暴露(104)晶面. 相反，$TM(OH)_x$在低温(≤300 ℃)下先热分解，形成无锂的$NiMnO_3$中间相，其生成的最终产物更倾向于(003)晶面的生长. 这些合成过程的差异直接反映在最终材料的微观颗粒架构上(图1(b)). 为精准量化这种差异，研究引入了PSD和PAR两个关键参数. 如图1(c), (f)所示，碳酸盐衍生富锂材料(CO3-LRLO)由近球形的一次颗粒组成，二次颗粒内部孔隙较多，表现出低PAR和低PSD(即高孔隙率)的特征. 氢氧化物衍生富锂材料(OH-LRLO)由近纤维状的一次颗粒紧密排列而成，内部孔隙极少，表现出高PAR和高PSD(即低孔隙率)的结构特征[23].

2.2 PSD主导的动力学与稳定性博弈

在动力学方面，CO3-LRLO极低的PSD导致其形成了丰富的多级孔隙结构，促进了电解液的深度浸润，丰富了液-固扩散路径. 因此，CO3-LRLO在5 C高倍率下能够展现出优异的放电容量(145.5 mAh/g，远高于OH-LRLO的114.7 mAh/g)(图2(a), (b)). 在结构与界面稳定性方面，电解液向二次颗粒内部的深度渗透，成倍增加了电极/电解液界面的比表面积(图2(c)). 在高压下，这不仅加剧了晶格氧的不可逆流失，还引发了高度活性的氧化态氧物种(O^{n-})对电解液的亲核攻击[24]. 剧烈的界面副反应加速了过渡金属的溶解和表面厚实CEI膜的生成. 更致命的是，低PSD导致的结构疏松在反复的体积收缩/膨胀中，极易引发贯穿二次颗粒的晶间微裂纹，并加速从层状向尖晶石/无序岩盐相的结构退化[23](图2(d)).

2.3 前驱体工程的总结

两类正极在界面稳定性、机械稳定性、扩散动力学、热稳定性上表现迥异. LRLO前驱体最优路线需结合应用场景、产业需求综合分析. 碳酸盐前驱体路线在于成本优势明显、Li^+扩散动力学优异，适合高功率但需通过电解液优化、包覆技术解决界面稳定性问题；氢氧化物前驱体路线在于体积能量密度、循环稳定性、热安全性更优，适合高安全/长寿命应用但需通过掺杂、复配方法弥补Li^+散动力学短板. 学界与产业界需重新评估LRLO正极前驱体选型策略，打破当前聚焦碳酸盐前驱体深度研究的单一范式，重视氢氧化物前驱体等路线的优势，进一步加速LRLO正极商业化进程.

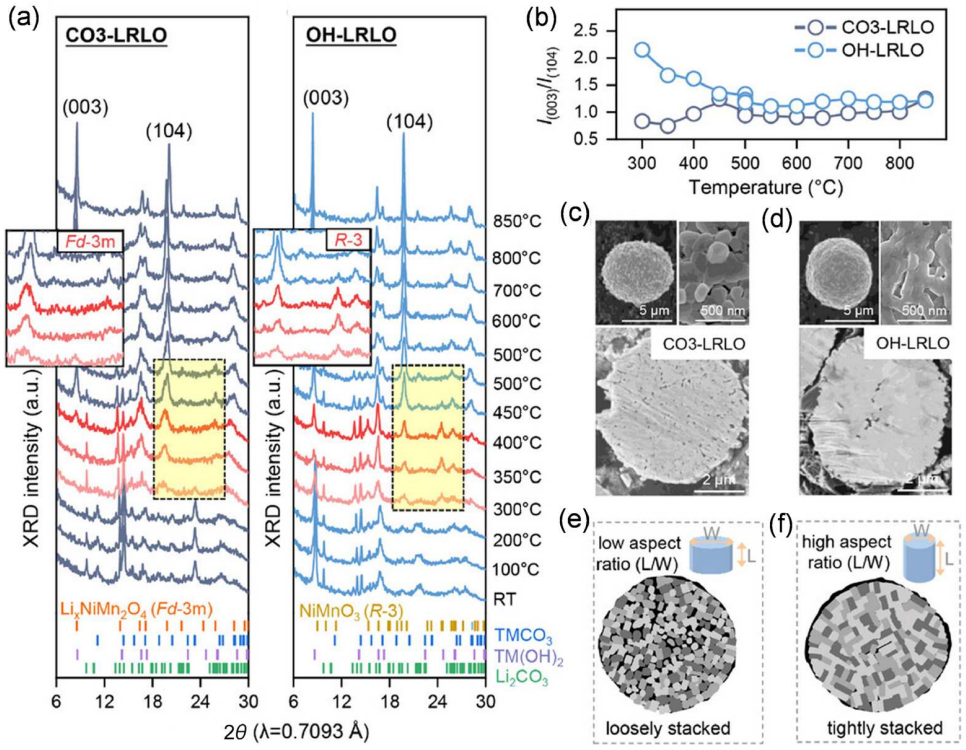


图 1 合成过程中的相演变差异及最终产物的微观结构对比[15]. 碳酸盐前驱体(a)与氢氧化物前驱体(b)和Li_2CO_3混合物的HT-XRD图谱. (c) 高温XRD测得的$I_{(003)}/I_{(104)}$峰强比随合成温度的变化曲线. CO_3-LRLO(d)与OH-LRLO(e)正极的表面及截面形貌. CO_3-LRLO(f)与OH-LRLO(g)正极中一次颗粒的纵横比及堆积密度示意图

Figure 1 Differences in phase evolution during synthesis and in the microstructure of the final product[15]. *In situ* HT-XRD patterns of (a) carbonate precursor and (b) hydroxide precursor mixtures with Li_2CO_3. (c) HT-XRD-measured $I_{(003)}/I_{(104)}$ ratio as a function of synthesis temperature. Surface and cross-sectional morphology of (d) CO_3-LRLO and (e) OH-LRLO cathodes. Schematic illustration of aspect ratio and stacking density of primary particles in (f) CO_3-LRLO and (g) OH-LRLO cathodes

3 化成激活协议: 容量与稳定性的博弈

在富锂层状正极材料的产业化进程中, 工作电压窗口的设定面临着严峻的权衡. 学术界通常采用2.0~4.8 V的宽电压区间来充分激发阴离子氧化还原反应[25], 但在实际工业应用中, 为了兼顾碳酸酯类电解液的稳定性和电池热安全性, 通常将常规工作电压的上限严格限制在4.5 V左右[26,27]. 然而, 这种受限的电压窗口会导致LRLO材料损失大量由阴离子氧化还原贡献的容量, 仅能发挥其理论容量的60%~70%. 尽管如此, 工业界对更高能量密度的持续需求, 推动了通过提高化成电压进行预活化的方法探索, 以期在2.5~4.5 V的温和工作电压区间内实现容量最大化. 这一特性为富锂层状正极材料所独有, 区别于镍钴锰酸锂、钴酸锂等传统层状氧化物正极材料(图3(a))[28,29]. 因此, 科学界对于富锂层状氧化物这类预活化工艺的影响仍存在诸多关键问题待解, 尤其是电化学预处理过程中的动态结构转变, 以及极端电压下的界面反应性, 这些问题直接阻碍了材料稳定性的可靠评估和电解液的优化设计[27,30].

3.1 容量激活机制: OM6配位环境的O4-O5转变

最新的多尺度表征研究系统揭示了高压化成对LRLO初始容量的巨大提升作用及其电子结构根源. 当化成电压从低压(low-voltage formation, LVF, 4.5 V)提升至高压(high-voltage formation, HVF, 4.8 V)时, 材料在后续2.5~4.5 V循环中的第二圈放电容量实现了21.6%的显著跃升(从172.46 mAh/g 增至 209.78 mAh/g)(图3(b)). 这种容量激增的本质在于高压驱动下的局部配位环境重构. 在4.8 V的深度脱锂状态下, 大量Li^+从过渡金属(TM)层中脱出, 产生了密集的锂空位, 从而极大降低了TM离子的迁移能垒, 促使TM发生显著的“面

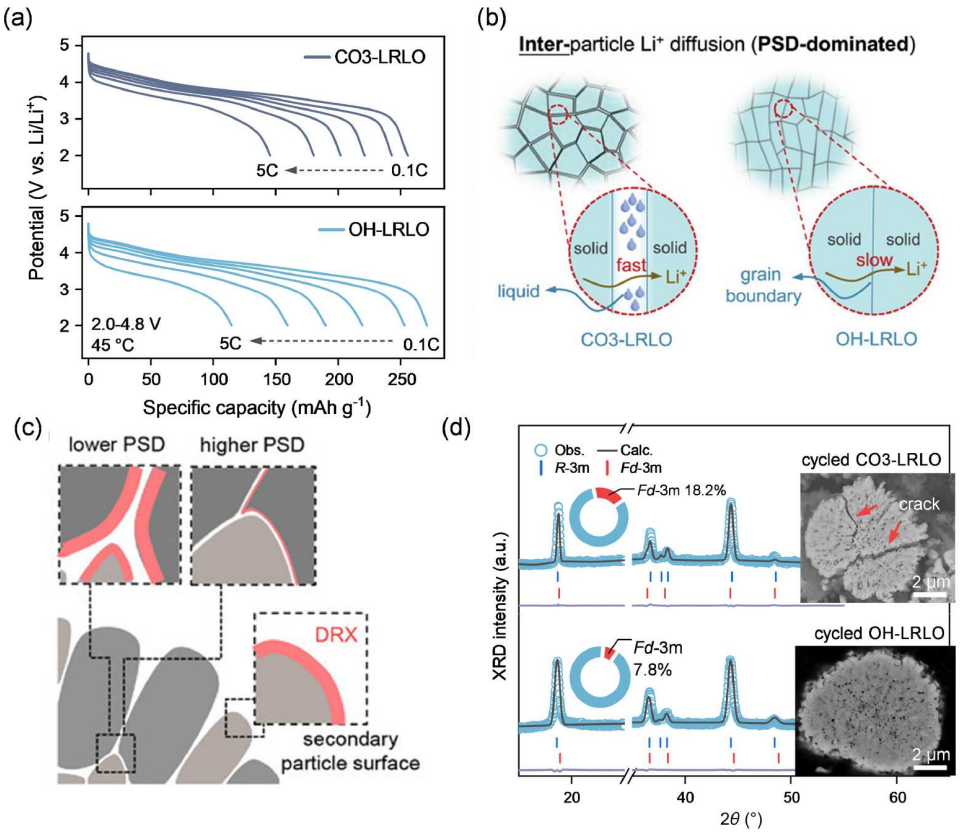


图 2 不同前驱体制备的LRLO的扩散动力学[15]. (a) 45℃、2.0~4.8 V条件下, OH-LRLO与CO3-LRLO正极的放电曲线. (b) 相应倍率性能. (c) PSD界面反应性之间的关联示意图. (d) 25℃、0.5 C、2.0~4.8 V下循环200次后电极片的XRD图谱与精修结果; 插图: 对应条件下循环200次后的截面SEM图

Figure 2 Diffusion kinetics of LRLO derived from different precursors[15]. (a) Discharge curves and (b) corresponding rate performance at different rates of OH-LRLO and CO3-LRLO cathodes at 45°C, 2.0–4.8 V. (c) Schematic diagram of the correlation between PSD and interface reactivity. (d) XRD patterns and refined results of electrode sheets after 200 cycles, 25°C, 0.5 C, and 2.0–4.8 V; insert: cross-sectional SEM image after 200 cycles

内迁移". 这种面内迁移驱动氧的配位环境(OM6, 其中M为阳离子)发生不可逆的相变, 即从初始的O4构型(OLi_xTM_2)向O5构型(OLi_yTM_1)演化. 相较于O4构型, O5构型的优势通过理论计算与态密度(DOS)分析表明, O5构型在费米能级附近具有更高的非键态轨道分布比例, 极大增强了过渡金属与氧(TM-O)的共价性. 此外, O5构型能够显著激活配体-金属电荷转移(LMCT)机制, 不仅促进了晶格氧的氧化还原活性, 还诱导了更多Ni和Mn阳离子参与放电过程中的电荷补偿, 实现了阴/阳离子氧化还原活性的协同增强[31](图3(c), (d)).

3.2 稳定性的代价: 面内迁移诱导的面外坍塌

尽管高压化成能够释放富锂层状正极材料诸多比容量, 但它也会对正极结构的稳定性带来破坏, 加速容量衰减. 长循环数据显示, 经过HVF激活的电池在200次循环后的容量保持率仅为79.14%, 较LVF协议(94.92%)大幅下降了15.8%(图3(b)). 失效的主导机制在于体相结构的退化, 而非单纯的界面反应. 虽然高压化成确实会导致一定程度的电解液分解加速(如CEI膜增厚及MnF_2的富集), 但这并非容量衰减的核心痛点. 真正的危机源于O4构型向O5构型转变过程中伴随的过渡金属迁移的级联效应. HVF导致的TM面内迁移和空位聚集, 极大地削弱了层间TM离子之间的静电斥力. 这种牵一发而动全身的层间环境, 使得TM离子更容易越过势垒, 发生面外迁移, 即从TM层不可逆地迁移至锂层(图4(a)), 最后表现为结构长程无序. 剧烈的面外迁移引发了严重的Li/Ni阳离子混排, 直接推动了有序层状结构向无序的尖晶石相或岩盐相转变. 这不

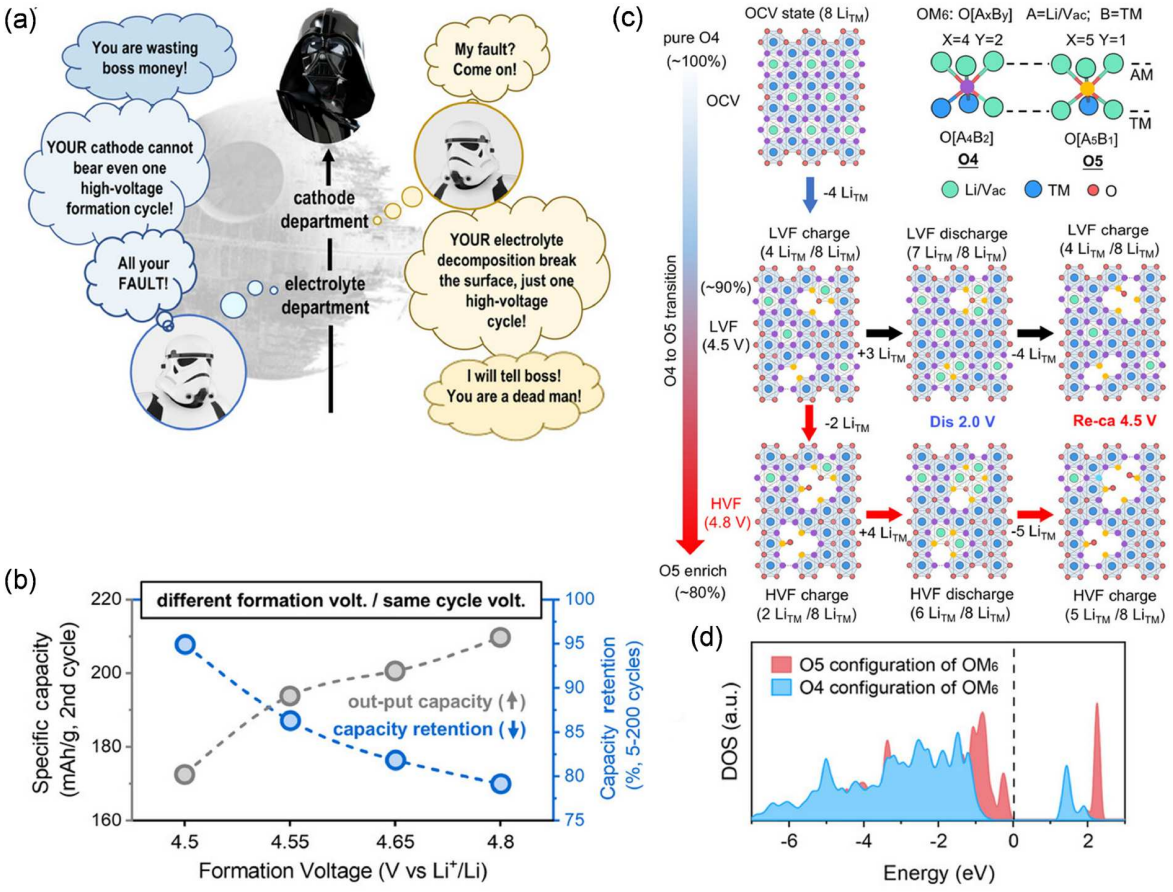


图 3 高压化成和低压化成条件下OM6结构演变的影响[17]. (a) 关于高压化成争议的卡通图. (b) 在不同的化成电压下, 锂半电池第二次循环的放电容量和5~200次的容量保持率. (c) 在531 eV激发能量下, 原始态、高压化成(HVF)与低压化成(LVF)样品第二循环充电至相同4.5 V时, LRLO的高分辨率高分辨率共振非弹性X射线散射(RIXS)谱; 插图: 0.125~2 eV区间的放大图与差分谱. (d) 原始的O4和O5 2p轨道的投影态密度(PDOS)

Figure 3 The influence of OM6 configuration evolution under HVF and LVF[17]. (a) Cartoon diagram of the controversy over high-voltage formation protocol. (b) Discharge capacity of the second cycle and capacity retention from 5 to 200 cycles for Li half-cell at different formation voltages. (c) High-resolution RIXS spectra recorded at an excitation energy of 531 eV for LRLO in the pristine and charged to the same 4.5 V for the 2nd cycle in HVF and LVF; inset: enlarged region from 0.125–2 eV region and the difference spectra. (d) The projected density of states (PDOS) of the O4 and O5 2p orbitals in pristine

仅引发了电压滞后, 更从物理空间上堵塞了Li^+的扩散通道, 导致锂离子扩散动力学(D_{Li+})的急剧恶化(图4(b), (c))[31~34].

3.3 化成激活协议总结

化成电压的博弈本质上是容量提升与结构稳定性之间的权衡. 探索LRLO材料在不同体系下的最佳化成电压区间有着重要意义. 现有研究表明, 采用多阶段化成工艺, 通过分段或梯度化成方案, 在不同电压阶段调控电流与时间, 能够以更温和的方式实现材料活化. 同时, 对LRLO颗粒进行表面包覆(如氧化铝、磷酸锂等惰性层)[35,36]或体相掺杂(如Ti、Mg等元素)[37~39], 可稳定材料表面与体相结构. 进一步抑制TM迁移, 减少晶格氧流失, 达到在高压化成后提升材料结构稳定性的效果. 此外, 通过电解液调控, 开发适配高电压体系的稳定电解液, 能够降低高电压下的副反应, 进一步保护材料表面结构.

4 工作电压区间: 放电深度的“异常”挑战

在将实验室级别的优异数据推向商业化应用的过程中, 评估电池在实际复杂工况下的可靠性是不可逾越的鸿沟. 在新能源汽车(energy vehicles, EV)或

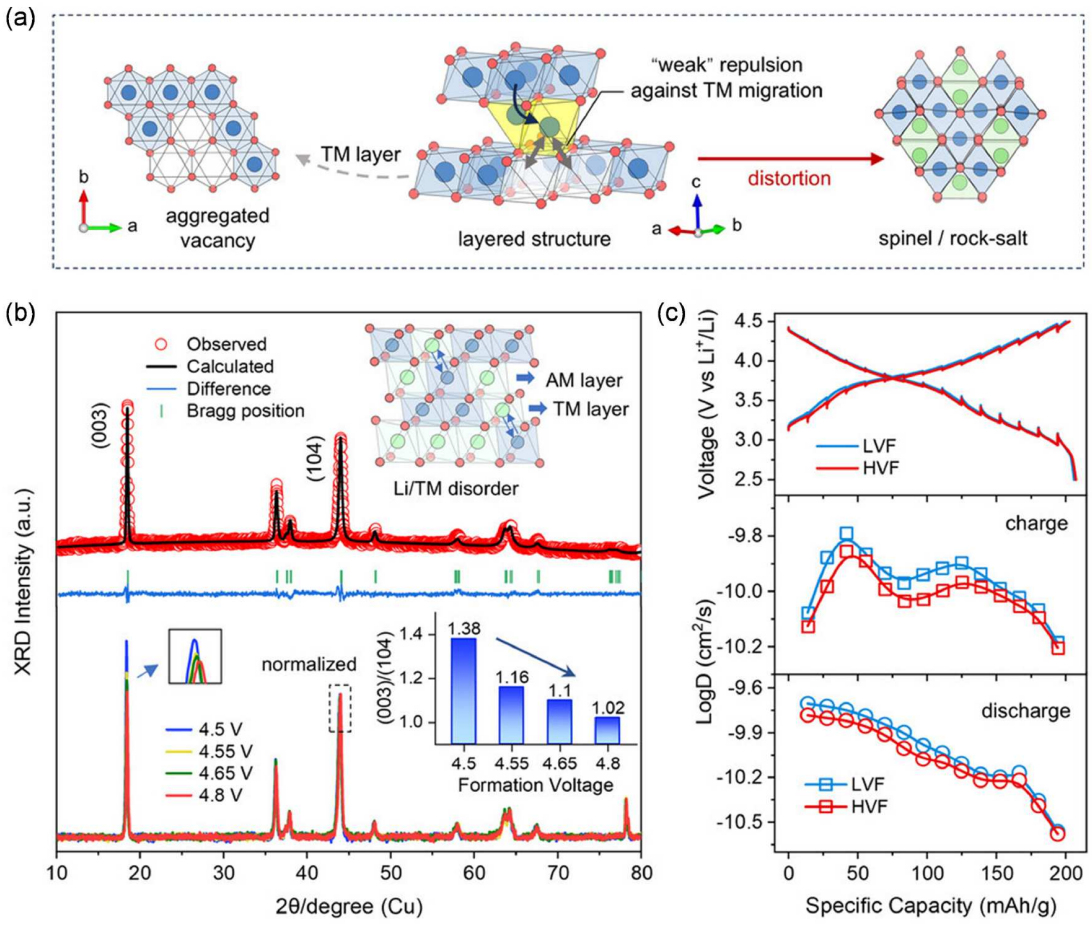


图 4 循环过程中层状结构的稳定性[17]. (a) 层状结构向尖晶石/岩盐相转变的示意图. (b) 不同化成电压下循环200周后的非原位XRD图谱与精修结果, 插图为(003)/(104)峰强比及(003)晶面放大图. (c) HVF与LVF样品循环100周后的恒流间歇滴定技术(GITT)电压曲线与锂离子化学扩散系数(log(D_{Li+}))

Figure 4 Stability of layered structure upon cycling[17]. (a) A schematic model illustrating phase changes from layered to spinel/rock salt. (b) *Ex situ* XRD patterns and refined results of different formation voltages after 200 cycles. Insets present the peak intensity ratio of (003)/(104) and the enlarged view of the (003) crystal plane. (c) Galvanostatic intermittent titration technique (GITT) voltage curve and chemical diffusion coefficient (log(D_{Li+})) of HVF and LVF cycling after 100 cycles

储能系统的实际运行中, 电池极少在100%的DOD下工作, 而是频繁处于浅充浅放的低放电深度(low depth-of-discharge, LDOD)状态. 然而, LRLO材料在不同DOD下的失效机制, 长期以来一直是学术界研究的"盲区"[40].

4.1 低放电深度下的加速衰减

在传统的层状正极材料(如NCM三元材料)中, 存在一个普遍共识: 循环电压区间越窄, 材料的结构应力越小, 循环寿命越长[41]. 然而, 最新的系统性评估揭示了LRLO材料一种"异常"的DOD依赖性衰减规律: 与NCM材料截然相反, LRLO在低DOD条件下的容量和电压衰减速度, 竟然远快于高DOD条件(图5(a)). 这种反常现象对LRLO的产业化构成了严峻挑战. 这意味着, 即便在实验室全电压范围(如2.0~4.8 V, 接近100% DOD)内测得了极佳的长循环寿命, 一旦搭载于实际设备进行常规的浅充浅放运行, 电池极易发生快速失效(图5(b)).

4.2 核心机制: 氧化态晶格氧(O^{n-})的累积效应

造成这种"反常"现象的根本原因, 在于LRLO材料特有的阴离子氧化还原反应的高电压迟滞与不对称性. 在充电过程的高电压阶段(>4.5 V), LRLO晶格中的氧离子(O^{2-})被氧化为高活性的氧化态氧(O^{2-}, $0 < n < 2$).

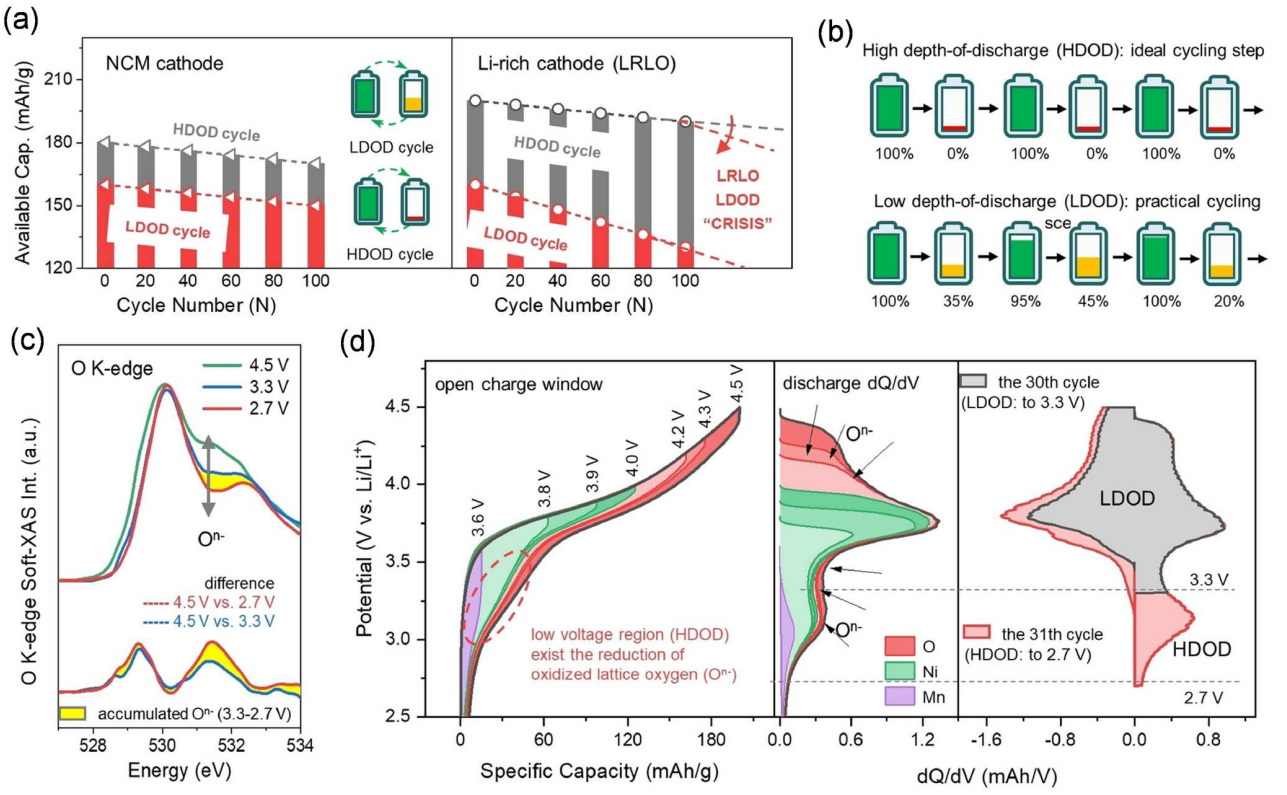


图 5 NCM与LRLO在不同放电深度下的容量衰减机制及电荷补偿行为[19]. (a) NCM和LRLO正极在高放电深度(HDOD)与LDOD长期循环下的可用容量衰减示意图, 插图为HDOD与LDOD循环模式. (b) 理想循环工况(HDOD)与实际循环场景(LDOD)模型. (c) LRLO首次放电过程中的OK边X射线吸收光谱(sXAS), 插图为差分谱. (d) 锂半电池中充电窗口从2.5~4.5 V逐步打开时的电压曲线及对应dQ/dV曲线, 右侧为3.3~4.5 V (LDOD)下第30圈与2.7~4.5 V(HDOD)下第31圈的dQ/dV曲线

Figure 5 The capacity decay mechanisms and charge compensation behaviors of NCM and LRLO under different discharge depths[19]. (a) The available capacity decay schematic illustrations of NCM and LRLO cathodes under HDOD and LDOD long-term cycling. Insert: HDOD and LDOD cycling models. (b) Models of ideal cycling step (HDOD) and practical cycling scene (LDOD). (c) O K-edge sXAS spectra of LRLO during the initial discharge process. Difference spectra are shown inset for clarity. (d) Voltage profiles and corresponding dQ/dV curves in Li half-cells as the charge window is opened stepwise from 2.5 to 4.5 V. The dQ/dV curves for the 30th cycle within the voltage ranges of 3.3–4.5 V (LDOD) and the 31st cycle within the voltage ranges of 2.7–4.5 V (HDOD) are on the right side

在随后的放电过程中, 这些O^{n-}的还原动力学极其迟缓, 通常需要在较低的电位下(<3.0 V)才能被完全还原回O^{2-}. 在HDOD下: 由于放电截止电压足够低, O^{n-}能够在每次循环结束时被充分还原, 晶格氧的氧化还原过程实现了闭环, 材料结构得以恢复. 在LDO下: 由于放电深度不足, 充电时产生的O^{n-}无法被完全还原. 随着循环次数的增加, 未还原的O^{n-}在LRLO晶格内部产生了严重"累积效应"[42](图5(c), (d)).

4.3 结构与界面的"级联崩塌"

循环中累积的高活性氧化态晶格氧(O^{n-}), 会引发一系列微观结构与界面的"级联崩塌". 首先是体相结构不可逆退化. 低DOD循环下, 放电不完全导致O^{n-}累积与过渡金属层中锂空位形成. 在LRLO中, 过渡金属层大量空位会破坏结构稳定性, 引发过渡金属迁移、空位团簇形成、配位数变化. 空位聚集形成的空位团簇极大地降低了过渡金属迁移的能垒, 驱动不可逆的"面外TM迁移". 这不仅导致了层状结构向尖晶石/岩盐相的加速相变, 更在物理空间上死锁了锂离子的三维扩散通道, 导致电荷转移阻抗急剧上升(图6(a)). 在界面副反应方面, 累积的O^{n-}具有极强的亲电性/亲核性, 当其扩散至颗粒表面时, 会对常规的碳酸酯类电解液发起强烈的亲核攻击. 这不仅导致了正极表面CEI膜的异常增厚, 加速了电解液的消耗, 还促进了过渡金属的大量溶出. 溶解的过渡金属离子伴随副产物迁移至负极, 破坏了固体电解质界膜的稳定性, 形成恶性循环,

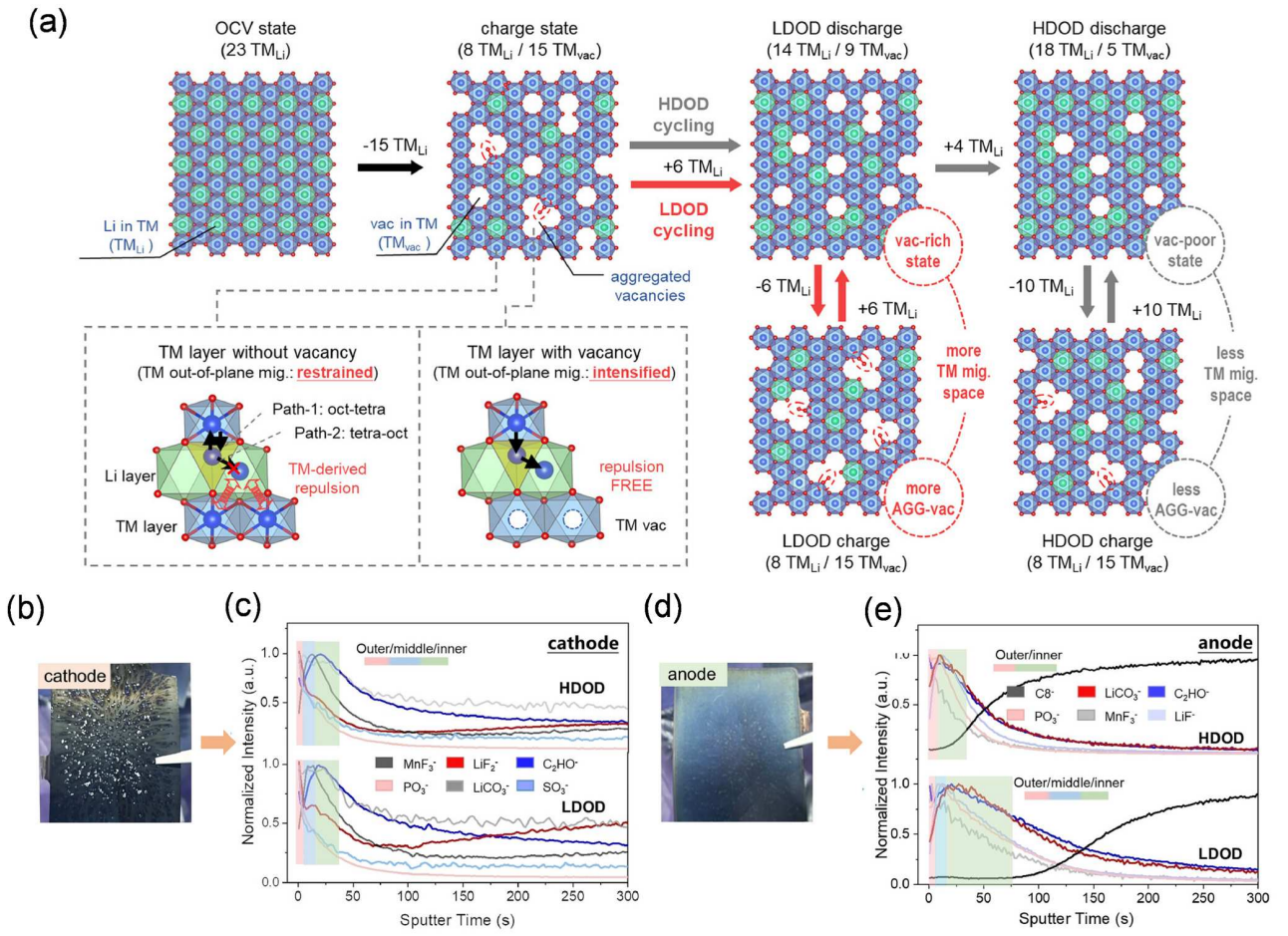


图 6 不同放电深度下的团簇演化、过渡金属迁移及全电池界面退化[19]. (a) 不同DOD下团簇的形成与演化示意图, 以及TM的面外迁移路径; 绿色为锂, 红色为氧, 蓝色为过渡金属; 黑色箭头表示锂位上的TM与TM层内TM之间的静电排斥作用. (b) LRLO软包全电池循环100次后的阴极退化形貌; (d) 阳极退化形貌. (c) HDOD/LDOD循环100次后阴极的飞行时间二次离子质谱(TOF-SIMS)表征, (e)为对应阳极的TOF-SIMS表征

Figure 6 Cluster evolution, transition metal migration and overall battery interface degradation under different discharge depths[19]. (a) The formation and evolution schematic illustrations of clusters and the out-of-plane migration pathways of TM during different DODs. Green, Li; red, O; blue, TM. The black arrow signifies the electrostatic repulsion between TM at Li sites and TM within the TM layer. The degradation of the cathode (b) and anode (d) in pouch-type full-cells of LRLO after 100 cycles. (c) Time-of-flight secondary ion mass spectrometry (TOF-SIMS) characterization of the cycled cathode and (e) anode electrodes after 100 cycles during HDOD and LDOD cycling

最终导致全电池系统的动力学瘫痪[42](图6(b)).

4.4 放电深度机制探究总结

DOD依赖性衰减机制的发现, 为LRLO的实际商业化应用指明了新的破局方向. 针对搭载LRLO材料的电池包, BMS的策略必须进行颠覆性调整. 应尽量避免电池长期处于高电位下的浅充浅放工况, 或者定期引入“深度放电校准”协议, 强制将累积的O^{n-}还原, 以恢复晶格活性并延长整体寿命. 在材料合成端, 需重点开发能够提高晶格氧可逆性的策略. 例如, 通过引入高电负性元素(如F掺杂)[43]或强配位金属离子[44], 增强TM-O共价性, 降低阴离子氧化还原的电压滞后, 使其在较高电位下也能实现快速还原.

5 总结与展望

富锂锰基层状氧化物(LRLO)的产业化, 面临着实验室“极限容量”与工业界“综合可靠性”之间的巨大鸿沟. 本文跳出常规的材料改性范畴, 从“合成制备—初始激活—实际运行”的全生命周期视角, 系统总结了LRLO走向商业化的三大底层逻辑与挑战. 首先是前驱体方面, 产业界必须锚定高堆积密度的氢氧化物前驱体路线, 以获取极致的长循环稳定性和力学完整性, 而

非盲目沿用追求初始动力学但结构脆弱的碳酸盐路线. 接着, 高压化成是激活枢纽, 高压化成虽能通过O4→O5配位转变激活阴/阳离子氧化还原, 但极易诱发过渡金属面外迁移导致结构坍塌. 寻求4.55~4.6 V的化成舒适区是现阶段兼顾容量与寿命的务实之举. 最后是从放电深度的角度, 实际应用中的浅充浅放会造成高活性晶格氧(O^{n-})的恶性累积, 引发远快于深度放电的“异常”衰减. 脱离实际工况的极限测试无法真实反映材料的服役寿命. 富锂层状正极材料未来的研究范式亟需作出改变, 要摒弃单一的理想全电压纽扣电池测试, 建立基于实际复杂工况的评估标准. 立足于氢氧化物前驱体, 集中攻关其动力学短板, 如开发梯度掺杂或新型外延包覆技术以疏通离子扩散通道. 解决LRLO的缺陷不能仅靠正极本身. 亟待开发抗亲核攻击的新型耐高压电解液, 并重构电池管理系统策略, 以化解O^{n-}的累积应力. 只有打破学术界与产业界的壁垒, 将原子级的机理探索与宏观的电池工程深度融合, 才能真正推动富锂层状正极材料迈向大规模商业化应用.

参考文献

1 Yang Y, Yang W, Yang H, et al. Electrolyte design principles for low-temperature lithium-ion batteries. eScience, 2023, 3: 100170
2 Tian Y, Lin C, Meng X, et al. Accelerated commercial battery electrode-level degradation diagnosis via only 11-point charging segments. eScience, 2025, 5: 100325
3 Li J C, Tang J, Tian J, et al. From oxygen redox to sulfur redox: a paradigm for Li-rich layered cathodes. J Am Chem Soc, 2024, 146: 7274–7287
4 Cui T, Liu L, Zhang J, et al. Beyond inducing anionic redox: controllable migration sequence of Li ions in transition metal layers toward highly stable Li-rich cathodes. Adv Mater, 2025, 37: 2412562
5 Chen N, Wang B, Liu Y, et al. The material influence factors on the actual capacity of lithium ion battery (in Chinese). Chin Sci Bull, 2018, 63: 3484–3493 [陈宁, 王博, 刘洋, 等. 影响锂离子电池实际容量的材料因素. 科学通报, 2018, 63: 3484–3493]
6 Wu X, Muhtar D, Zhang D, et al. Progress of high energy density cathode materials for lithium-ion batteries (in Chinese). Chin Sci Bull, 2023, 69: 3024–3046 [吴雪敏, 迪力夏提·木合塔尔, 张朵朵, 等. 锂离子电池高能量密度正极材料的研究进展. 科学通报, 2023, 69: 3024–3046]
7 Li Q, Zhou D, Zhang L, et al. Tuning anionic redox activity and reversibility for a high-capacity Li-rich Mn-based oxide cathode via an integrated strategy. Adv Funct Mater, 2019, 29: 1806706
8 Park G T, Kim S B, Namkoong B, et al. A new ternary Co-free layered cathode, $Li[Ni_{1-x-y}TiAl]O_2$, for high-energy lithium-ion batteries. Mater Today, 2023, 71: 38–49
9 Jiang Z, Zhang K, Ding Q, et al. Metal–ligand spin-lock strategy for inhibiting anion dimerization in Li-rich cathode materials. J Am Chem Soc, 2025, 147: 3062–3071
10 Zhao X, Chen Y, Cao X, et al. Research progress in cathode materials of secondary batteries with high specific energy based on anionic charge compensation mechanism (in Chinese). Chin Sci Bull, 2024, 70: 1118–1131 [赵晓雯, 陈毅龙, 曹鑫, 等. 基于阴离子电荷补偿机制的高比能二次电池正极材料研究进展. 科学通报, 2024, 70: 1118–1131]
11 Yang Y, Luo T, Zuo Y, et al. Expandable fast Li-ion diffusion network of Li-rich Mn-based oxides via single-layer $LiCo(Ni)O_2$ segregation. Adv Mater, 2025, 37: 2414786
12 Seo D H, Lee J, Urban A, et al. The structural and chemical origin of the oxygen redox activity in layered and cation-disordered Li-excess cathode materials. Nat Chem, 2016, 8: 692–697
13 Okubo M, Yamada A. Molecular orbital principles of oxygen-redox battery electrodes. ACS Appl Mater Interfaces, 2017, 9: 36463–36472
14 Jiao S, Wang J, Hu Y S, et al. High-capacity oxide cathode beyond 300 mAh/g. ACS Energy Lett, 2023, 8: 3025–3037
15 Liu J, Bao Z, Cui Y, et al. Pathways for practical high-energy long-cycling lithium metal batteries. Nat Energy, 2019, 4: 180–186
16 Assat G, Tarascon J M. Fundamental understanding and practical challenges of anionic redox activity in Li-ion batteries. Nat Energy, 2018, 3: 373–386
17 Zhang H, Liu H, Piper L F J, et al. Oxygen loss in layered oxide cathodes for Li-ion batteries: mechanisms, effects, and mitigation. Chem Rev, 2022, 122: 5641–5681
18 Ma R, Liu J, Wang S, et al. Progress on thermal runaway propagation characteristics and prevention strategies of lithium-ion batteries (in Chinese). Chin Sci Bull, 2021, 66: 2991–3004 [马瑞鑫, 刘吉臻, 汪双凤, 等. 锂离子电池热失控扩展特征及抑制策略研究进展. 科学通报, 2021, 66: 2991–3004]
19 Seo M G, Han S M, Jo H J, et al. Strategic synthetic pathway for tailoring the crystallographic and microstructural evolution of cathode materials for Li-ion batteries. ACS Energy Lett, 2026, 11: 4084–4093
20 Lee D, Kim H, Jeong S M. Unveiling the future of Li-ion batteries: real-time insights into the synthesis of advanced layered cathode materials. ACS

Energy Lett, 2024, 9: 4255–4264
21 Li H, Wang L, Wang J, et al. Layered-to-layered synthesis of high-performance nickel-rich layered cathodes via low-temperature oxidation of layered hydroxide precursor. Adv Energy Mater, 2025, 15: 2500325
22 Gu Y, He S, Wang K, et al. Dual-gradient structural design for synchronized phase transitions and stress-resilient O3-type sodium cathodes. ACS Nano, 2026, 20: 7956–7966
23 Huang Y, Li C, Zhang K, et al. How does the precursor influence the Li-rich layered oxide cathode? Angew Chem Int Ed, 2025, 64: e18277
24 Zhang B, Zhang H, Luo H, et al. Manipulated fluoro-ether derived nucleophilic decomposition products for mitigating polarization-induced capacity loss in Li-rich layered cathode. Angew Chem Int Ed, 2024, 63: e202316790
25 Zhang B, Zhang Y, Wang X, et al. Role of substitution elements in enhancing the structural stability of Li-rich layered cathodes. J Am Chem Soc, 2023, 145: 8700–8713
26 Ren M, Jiao S, Zhao Y, et al. Thermal decomposition mechanisms and inherent stability differences between O2- and O3-lithium-rich manganese-based oxide cathodes. Adv Funct Mater, 2025, 36: e30009
27 Zuo P, Abraham D P, Wang C. Origin of electrochemical activation leading to enhanced cycling stability of Li- and Mn-rich cathodes. Angew Chem Int Ed, 2026, 65: e8818196
28 Li X, Zhu X, Zhang Y, et al. Ternary inert element co-doping: a new approach to stable 4.7 V $LiCoO_2$. Adv Mater, 2025, 37: 2506228
29 Eum D, Ramachandran H, Sun T, et al. Uniform pore structure enables negligible degradation in undoped and uncoated Ni-rich cathodes. Nat Energy, 2026, 11: 593–602
30 Jiao C, Zheng Q, Zhang K, et al. Regulating interfacial nucleophilic chemistry via hybrid electrolyte enables stable 4.8 V-class Li-rich||Li-metal batteries. ACS Nano, 2025, 19: 35141–35153
31 Zhang K, Zheng Y, Yin J, et al. Unveiling the influence of formation voltage on Li-rich layered oxide cathode. Angew Chem Int Ed, 2025, 64: e202515719
32 Li B, Sougrati M T, Rousse G, et al. Correlating ligand-to-metal charge transfer with voltage hysteresis in a Li-rich rock-salt compound exhibiting anionic redox. Nat Chem, 2021, 13: 1070–1080
33 Li B, Zhuo Z, Zhang L, et al. Decoupling the roles of Ni and Co in anionic redox activity of Li-rich NMC cathodes. Nat Mater, 2023, 22: 1370–1379
34 Wang S, Mei Y, Su J, et al. Decoding the oxygen activity with iron through ligand-to-metal charge transfer in Li-rich layered cathodes. J Am Chem Soc, 2025, 147: 47911–47920
35 Yan Y, Fang Q, Kuai X, et al. One-step surface-to-bulk modification of high-voltage and long-life $LiCoO_2$ cathode with concentration gradient architecture. Adv Mater, 2023, 36: 2308656
36 Cheng X, Wang Y, Lu J, et al. Regulating oxygen redox reactions in lithium-rich materials *via* an Al_2O_3-doped ZnO layer for enhanced stability and performance. J Mater Chem A, 2024, 12: 32871–32884
37 Guo W, Yu H, Wang M, et al. Compositional gradient design of Ni-rich Co-poor cathodes enhanced cyclability and safety in high-voltage Li-ion batteries. ACS Nano, 2025, 19: 8371–8380
38 Yu R, Banis M N, Wang C, et al. Tailoring bulk Li^+ ion diffusion kinetics and surface lattice oxygen activity for high-performance lithium-rich manganese-based layered oxides. Energy Storage Mater, 2021, 37: 509–520
39 Wu T, Zhang X, Li Y, et al. Quantitative identification of dopant occupation in Li-rich cathodes. Adv Mater, 2024, 37: 2408543
40 Liu H, Li C, Hu X, et al. Multi-modal framework for battery state of health evaluation using open-source electric vehicle data. Nat Commun, 2025, 16: 1137
41 Shen J, Tian X, Li Z, et al. Enhancing high-temperature electrochemical performance of single-crystal ultra-high nickel cathodes via high-valence Nb gradient doping. Adv Funct Mater, 2026, 36: e25784
42 Zhang K, Chen Y, Zhu Y, et al. Depth-of-discharge dependent capacity decay induced by the accumulation of oxidized lattice oxygen in Li-rich layered oxide cathode. Angew Chem Int Ed, 2024, 64: e202419909
43 Sun X, Qin C, Zhao B, et al. A cation and anion dual-doping strategy in novel Li-rich Mn-based cathode materials for high-performance Li metal batteries. Energy Storage Mater, 2024, 70: 103559
44 Hu K, Tang H, Zheng B, et al. Constructing targeted strong $Nb_{4d}-O_{2p}-Li_{2s}$ configurations to obtain excellent energy density and long life for Li-rich cathodes. Angew Chem Int Ed, 2025, 64: e202413563

Summary for “富锂层状正极材料产业化的关键挑战与进展”

Critical challenges and recent advances in the commercialization of lithium-rich layered cathodes

Zongliang Dai[1] & Yu Qiao[2*]

[1] *SDU-ANU Joint Science College, Weihai 264209, China*
[2] *State Key Laboratory of Physical Chemistry of Solid Surfaces, Xiamen University, Xiamen 361005, China*
* Corresponding author, E-mail: yuqiao@xmu.edu.cn

Driven by the booming electric vehicle and grid energy storage markets, demand for high-energy-density lithium-ion batteries continues to surge. Conventional layered cathodes, whose practical capacity is approaching the theoretical limit, can barely meet future performance requirements. Lithium-rich layered oxides (LRLOs), leveraging both cationic and anionic redox reactions, boast a theoretical specific capacity exceeding 300 mAh/g and are widely recognized as the most promising next-generation cathode system. Nevertheless, LRLO commercialization is hindered not only by well-documented issues such as voltage fade, oxygen release and initial capacity loss, but more critically by the profound disconnection between academic research and industrial practice. Most laboratory studies rely on carbonate precursors, wide voltage windows and full-depth cycling, which deviate significantly from the hydroxide precursor routes, 4.5 V operating voltage and shallow charge-discharge conditions adopted in industry. This mismatch has become a major bottleneck for translating fundamental advances into real-world applications. To bridge this gap, this review systematically summarizes recent progress in LRLO commercialization from three core lifecycle dimensions: precursor engineering, formation activation protocols, and depth-of-discharge (DOD) effects under practical operating conditions.

First, we elucidate the decisive role of precursor selection in shaping LRLO microstructural architecture and electrochemical performance. The fundamental disparity between carbonate-derived (CO3-LRLO) and hydroxide-derived LRLOs (OH-LRLO) stems from the primary-particle stacking density (PSD) inherited from distinct sintering phase evolution pathways. CO3-LRLO with low PSD features abundant pore networks and favorable Li^+ diffusion kinetics, delivering excellent 5 C rate capability. However, deep electrolyte infiltration caused by low PSD aggravates interfacial side reactions, lattice oxygen loss and intergranular cracking, accelerating structural degradation. In contrast, OH-LRLO with high PSD achieves superior cycling stability, thermal safety and volumetric energy density despite slightly compromised rate performance. We clarify applicable scenarios for each route and highlight the necessity of shifting research focus to hydroxide precursors to align with industrial demands.

Second, this review dissects the trade-off between capacity activation and structural stability regulated by formation voltage. To offset capacity loss under the industrial 4.5 V operating window, 4.8 V high-voltage formation (HVF) is widely employed to pre-activate anionic redox activity. The underlying mechanism is the irreversible O4-to-O5 coordination transition driven by in-plane transition metal migration, which enhances TM-O covalency and triggers synergistic cationic-anionic redox, boosting subsequent discharge capacity by 21.6%. Nevertheless, HVF weakens interlayer electrostatic repulsion and induces irreversible out-of-plane transition metal migration, accelerating layered-to-spinel/rock-salt phase transformation and deteriorating long-cycle stability. A moderate formation voltage of 4.55–4.6 V is proposed as a pragmatic compromise to balance capacity output and structural durability.

Third, we reveal the anomalous accelerated degradation of LRLOs under low-DOD (LDOD) cycling, contrary to conventional NCM cathodes where narrower voltage windows extend cycle life. The root cause lies in the pronounced voltage hysteresis of anionic redox: oxidized lattice oxygen species (O^{n-}, $0 < n < 2$) generated during charging cannot be fully reduced at high discharge cut-off voltages, leading to continuous accumulation of reactive O^{n-} in the lattice. This accumulation triggers a cascade of failures, including aggravated transition metal migration, bulk structural degradation and severe nucleophilic electrolyte attack, ultimately causing faster capacity and voltage fade than high-DOD cycling. Corresponding mitigation strategies are proposed, including periodic deep-discharge calibration via battery management systems and enhanced oxygen redox reversibility via elemental doping.

Overall, this review provides a holistic perspective on LRLO commercialization spanning material synthesis to practical operation. We emphasize that future research should abandon idealized full-voltage coin-cell testing and establish evaluation standards based on real-world operating conditions. Coordinated optimization of precursor engineering, anti-nucleophilic electrolyte design and battery management strategies will be critical to breaking current bottlenecks and promoting the large-scale application of LRLO cathode materials.

lithium-rich layered oxides, precursor, primary-particle packing density, formation voltage, depth-of-discharge

doi: 10.1360/CSB-2026-0653